

Integrating Pixel-Based Algorithms for Area Measurement in Brain Tumor Classification

Dwi Swasono Rachmad

Department Information Technology, Faculty of Computer Science, Bhayangkara University,
Jakarta, Indonesia

Email: dwi.swasono@dsn.ubharajaya.ac.id

Abstract

Diagnosing brain cancers in medicine necessitates an examination utilizing magnetic resonance imaging (MRI). picture processing techniques in the medical domain are integral to computed tomography detection in MRI due to their excellent picture fidelity and little radiation exposure. Nonetheless, there remain deficiencies in the interpretation, analysis, and imaging of brain tumors in detection. This study seeks to identify brain tumors to ascertain their size and extent by a pixel-based methodology. The dataset utilized originates from Cipto Mangunkusumo Hospital in Jakarta and comprises T1 contrast and BMP sequences. The research procedure will employ many methodologies, including active contours, Otsu's method, and a combination of techniques, with comparisons utilizing the MRI MicroDicom viewer. The image testing phase utilizing Matlab and Python with thirteen image datasets. The findings from this study, which involved segmentation and extraction techniques to quantify the area of brain tumors using a pixel-based approach, indicate that the combined method outperforms alternative methods by achieving superior accuracy of 99%. Other methods fail to attain this level of accuracy, and the combined method also demonstrates optimal error differentiation in template matching.

Keywords

Brain Tumor, Merge, MRI, Pixel, Template Matching

Introduction

The domain of computer science and communication is intricately linked to human labor (Vauzia & Sumitra, 2020). Because of the technological developments that have been made in the field of communication media, which are founded on the principles of information technology (Finch et al., 2021). Computer media has exhibited a diverse range of sizes, spanning from compact devices to expansive systems, all showcasing remarkable performance capabilities (Faria et al., 2017) (Sasvari, 2013) (Parihar, 2018). In addition, technology has greatly enhanced different areas

Submission: 12 March 2025; **Acceptance:** 12 June 2025; **Available Online:** June 2025



Copyright: © 2025. All the authors listed in this paper. The distribution, reproduction, and any other usage of the content of this paper is permitted, with credit given to all the author(s) and copyright owner(s) in accordance with common academic practice. This article is an open access article distributed under the terms and conditions of the Creative Commons Attribution (CC BY) license, as stated in the website: <https://creativecommons.org/licenses/by/4.0/>

of human labor by enabling faster, more efficient, and more economical operational operations (Skaržauskienė et al., 2013).

Previously, healthcare professionals employed manual approaches and utilized MRI provider viewer programs, alongside mathematical morphology integrated inside computational analyses, to quantify the residual components of the tumor that necessitated manual measurement, particularly the diatarsis. Nonetheless, due to the diverse shapes, sizes, and depths of the tumors in this instance, the pictures acquired during the identification process via MRI remain insufficiently precise for accurately locating brain tumors in MRI scans. In computer science, manual research methods are obsolete; so, researchers must execute numerous processing operations on pictures obtained from MRI detection. At now, there has been no implementation of detection utilizing a pixel-based approach with BMP format, which facilitates data processing without compromising the integrity or attributes of the MRI image dataset.

The forthcoming research will expand upon prior studies to analyze and evaluate MRI image measurements through a pixel-by-pixel methodology utilizing a BMP type MRI Contrast T1 sequence dataset.

To streamline the investigation of therapy treatments and clinical trials, a succinct and thorough evaluation of glioma images is essential (Irianto et al., 2024). Given these circumstances, establishing a volume size approach appears to be a prudent decision. The significance of progress, consistency, and accessibility of segmentation tactics is paramount. This study demonstrates a robust association between the mathematical morphological formula of the ellipsoid and segmentation in accurately estimating the volume of glioma brain tumor divisions (Parney & Prados, 2005). This relationship will facilitate accurate observations of the patient's therapy response, as categorized by the four RANO groups. The findings indicate that the ellipsoid formula is advantageous for measurements in clinical contexts (Le Fèvre et al., 2022). Hematoma size and individual variations in mathematical morphology can influence the application of the Tada technique for assessing intracerebral hemorrhage (ICH) (Swati et al., 2019). The volume measurement range of 20-40 ml may suggest diminished observer reliability, resulting in possible mistakes in illness evaluation and treatment. Addressing the aforementioned constraints and enhancing the precision of the measured values (Gong et al., 2021) is crucial for assessing two distinct methodologies for quantifying intracerebral hemorrhage (ICH) volume (Hasan et al., 2022). The two employed methods are software-assisted planimetry and the elliptical volume approach, referred to as ABC/2. Section (Jolink et al., 2020) (Maeda et al., 2013).

A multitude of methods for viewing tumor volumes are elucidated in a series of current scientific studies (Feldman et al., 2014), the process starts with the exploitation of a number of photographs, both one-dimensional and two-dimensional. Through the use of mathematical computations and mathematical morphological calculations of hemi-ellipsoids, a number of earlier research have demonstrated that it is possible to provide representations of the three-dimensional shape of tumors. To determine three crucial dimensions, namely height (Ben Abdallah et al., 2016), breadth, and length, it is necessary to have estimates of tumor volume (Sápi et al., 2015).

The authors describe a novel system for classifying hemi-ellipsoid brain tumors. This methodology employs mathematical morphology, the active contour technique, Otsu's method

(Mittal et al., 2017), fundamental morphological operations, and data extraction (Parveen & Singh, 2015). This study indicates that the prior mathematical technique is inferior; yet, a pixel-based approach is necessary in the realm of computer science. The deficiencies of the employed algorithm, as well as inaccuracies in comparisons between algorithms and the matching of tumor area objects from the analyzed algorithms, remain undetermined. Utilization of pixel size (Kumar & Tiwari, 2019) as a criterion for differentiating various cancer kinds. The shape generated using the Otsu algorithm, active contour (Hadi et al., 2022), and calculations from the Microdicom application (Müller et al., 2004) will be employed in the evaluation process, alongside merge two algorithms (Shukran et al., 2021), particularly for classifying items based on the detection of brain tumors (Bangare et al., 2017).

Methodology

The researcher goes through a number of stages during the process of conducting research. These stages include determining the dataset that will be used, creating ground truth as the baseline value, and then moving on to segmentation of the active contour image, Otsu, and hybrid. Additionally, the researcher uses calculations with an MRI viewer application called MicroDicom after completing these stages. The following are the requirements that are associated with each of these methods:

This analysis employs magnetic resonance imaging (MRI) data sourced from the Research and Development Center of Cipto Mangunkusumo General Hospital (Mehmet Kocak, 2022). This dataset provides statistics on the prevalence of cerebrovascular disorders. The data (Madhupriya et al., 2019) (Sreenivasan et al., 2016) comprises a compilation of clinically acquired information regarding brain tumors from the Radiology Department of Cipto Mangun Kusumo General Hospital in Jakarta, Indonesia. A skilled neuroradiologist (Sreenivasan et al., 2016) is necessary to regularly update the dataset and furnish ground truth labels. Upon acquisition, the magnetic resonance imaging (MRI) pictures are digitized and archived. Figure 1 presents a collection of images from the inquiry.

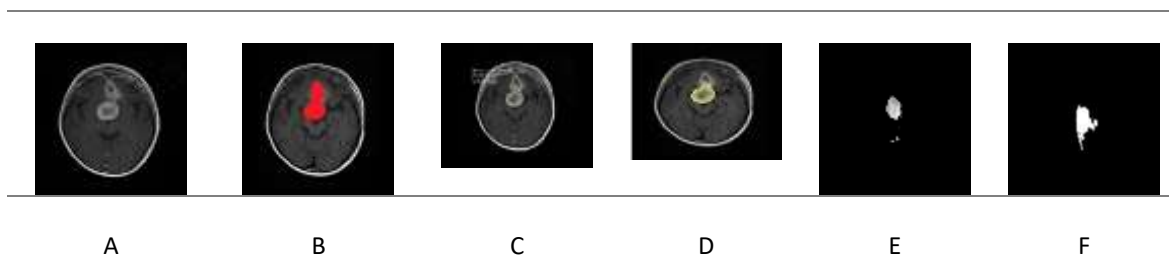


Figure 1 Original MRI (A), Ground Truth (B), Microdicom (C), Active Contour (D), Otsu (E), Combine(F)

This study's design has three primary phases: Saving photos in BMP format (Jones & Rabbani, 2020). (2) Establishing ground truth (Wang et al., 2019) as a primary reference for future comparisons with alternative methods (Yang et al., 2015) (3) Employing active contour, Otsu, and merge two algorithms integrated with advanced morphological processes (Vaillant & Davatzikos, 1997) for brain tumor segmentation, in conjunction with computations utilizing the

microdecom application. Multiple procedures are employed, commencing with the determination of the ground truth and necessitating significant computations utilizing tools such as microdecom viewer, Otsu, active contour, and merge two methods. These methods are frequently employed to derive statistical data from photographs. Moreover, the extraction methodology takes into account the pixel dimensions pertinent to each technique

Dataset

This method necessitates the provision of precise and verified data concerning the specific location of the tumor seen in the image (Wongso et al., 2017) (Gunawan et al., 2018). This information will function as training data and criteria for assessing diverse research procedures, including manual mathematical morphology, pixel-based segmentation and extraction techniques devoid of operator intervention, and template matching algorithms. Moreover, image sections are meticulously delineated to differentiate the primary subject of interest from the adjacent backdrop (Isunuri & Kakarla, 2019)

Segmentation

Magnetic resonance imaging (MRI) segmentation is employed to delineate regions exhibiting distinct features that signify the existence of cerebral cancer. The active contour method is employed to segment pre-processed MRI images. Figure 1 employs the Original Image, active contour, and fusion techniques to identify brain cancer (Widodo et al., 2016).

Extraction

Extraction is the primary phase necessary for acquiring comprehensive information from the image under examination.

a. Create Ground Truth

Calculations utilizing ground truth data are employed to derive baseline values obtained from other methodologies (Example, n.d.) (Iskhakov, 2016). The provided MRI image (Figure 1B) will act as a benchmark for comparison with alternative techniques. The ground truth will be determined, and a designated tumor location has been established as the baseline value (Kumari et al., 2020).

b. Dataset obtained from the Microdicom application

This dataset is sourced from original MRI data acquired with the Microdicom MRI viewer. The MRI images presented (Figure 1 C) were produced by processing the dataset with the MicroDicom program. This program offers functionalities that facilitate users in assessing the dimensions of the tumor region.

c. Dataset derived from active contours

This technology employs active contours as a segmentation technique, utilizing closed curves that can dynamically expand or contract to precisely delineate the image. The active contour method has been employed to segment MRI images, with contours modified to align with the location of specific brain tumors for detection purposes (Figure 1 D).

d. Dataset derived using the Otsu algorithm

This methodology employs the Otsu method for segmentation. This method computes the image intensity distribution and image weight, yielding a threshold value of 256. Upon alteration of the image value in the subsequent study, the image will be modified to white. This is the preliminary MRI image for analysis.

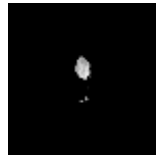


Figure 2 Outcomes of Otsu's MRI methodology

Image 2 illustrates the Otsu segmentation method, succeeded by the extraction phase employing the Otsu 256 thresholding technique, culminating in contour detection. This process entails delineating a bounding box around the tumor and marking it in blue to facilitate differentiation between images with and without the tumor.

e. Merge Algorithm-Based Datasets



Figure 3 Merge two algorithm MRI results

The two fusion techniques encompass multiple operations, including picture capture and the application of acoustic thresholding in conjunction with the active contour method. The technique commences with the preliminary acquisition of MRI images. The Otsu thresholding method is subsequently employed to provide labels to items within the image. Ultimately, active contours are employed for picture segmentation. The subsequent method employs the active contour technique for detection. This method recognizes analogous images and adjusts them to the specified image objects for detection.

Pixel calculation

This treatment employs various techniques, including microdicom MRI viewing software, the Otsu method, active contouring, and their integration. The subsequent actions are executed:

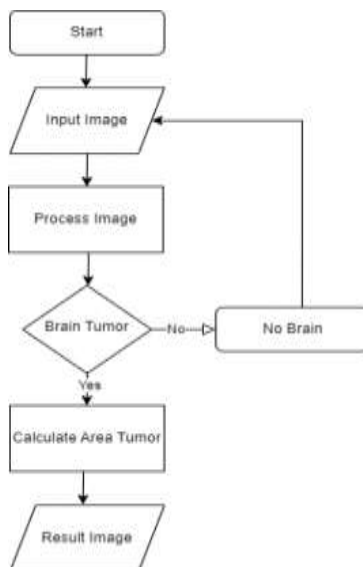


Figure 4 Measurement Technique Electrical Schematic

The aforementioned procedures encompass the primary techniques of segmentation and extraction utilizing Microdicom, Otsu's method, active contour, and the integration of these approaches with a pixel-based methodology approach.

Template Matching Algorithm

At this level, the technique will employ the pixel-based pattern matching algorithm derived from segmentation processing. Pixel extraction will be conducted via multiple techniques, including ways employing microdicom software, active contours, Otsu's method, and the integration of two methodologies. The chosen method will rely on the ground truth as a benchmark value. Subsequent to the implementation of the strategy, the ensuing procedure will employ the pixel pattern matching algorithm (Hashemi & Aghdam, 2016).

The survey entails comparing each pixel in the digital picture matrix with a template image with this technique. Template matching employs the equation:

$$r = \frac{\sum_{k=1}^N (x_{ik} - \bar{x}) \cdot (y_{jk} - \bar{y})}{\sqrt{\sum_{k=1}^N (x_{ik} - \bar{x})^2 \cdot \sum_{k=1}^N (y_{jk} - \bar{y})^2}} \quad (1)$$

The correlation coefficient, represented as r , quantifies the relationship between two variables. In this instance, x_{ik} denotes the reference image, whereas \bar{x} signifies the mean value of the image.

Algorithm error

Accuracy is typically defined as the extent of divergence of a quantitative measurement from the true value (“Numerical Methods 5.1. Introduction,” 1998). Error analysis is crucial while doing calculations with numerical methods. The error size quantifies the precision of a numerical solution, indicating its proximity to the accurate result.

True value = Approximation + Error If the margin value relative to the true value is a, then the discrepancy is termed Error.

In numerical engineering, failure, commonly referred to as error, signifies the divergence between an actual value and the value produced by an iterative process intended to approach the true value. The error can be substantially reduced, producing results that are adequately close to the genuine value, or possibly insignificant.

In numerical engineering, accuracy can be evaluated using two distinct metrics: absolute error and relative error. The absolute error is the magnitude of the difference between the true value of x and the measured value of x'.

$$\epsilon_A = |x - x'| \quad (2)$$

The relative error is determined by dividing the difference between the real value of x and the observed value x' by the actual value, rather than the absolute error. The outcome is a dimensionless quantity. The formula for relative error is presented below.

$$\epsilon_R = \left| \frac{x-x'}{x} \right| 100\% \quad (3)$$

Precision refers to the number of measurements conducted under identical conditions, yielding consistent outcomes. In this instance, the computation of absolute error and relative error in numerical approaches is as follows:

1. Error Absolutely

$$\epsilon_A = |357 - 1008|$$

2. Error Relative

$$\epsilon_R = \left| \frac{357 - 1008}{357} \right| 100\%$$

3. Percentage

Formula:

$$\text{Accuracy} = \frac{\text{Ground Truth Value}}{\text{Value Obtained}} 100\%$$

or

$$\text{Accuracy} = 100\% - \text{Value Obtained}$$

The researcher will employ a hybrid approach, integrating multiple methods, including the Otsu algorithm, active contour algorithm, and measurements utilizing the Microdicom viewer application, to achieve optimal results in addressing errors or low accuracy values. The hybrid algorithm integrates Otsu and active contour, as the researcher identified an effective technique by merging the two methodologies. Subsequently, after executing the image processing on MRI using hybrid algorithms based on testing and error analysis to determine the optimal and minimal error values, the process proceeded with template matching to align the MRI images.

Results and Discussion

Results must be displayed in a coherent order using text, tables, graphs, and figures; redundancy in presenting identical data in several formats should be eschewed. The results discussion must delineate and elucidate the observed phenomena, trends, optimal values, and additional information that demonstrates the correlation between these results and those derived from prior, analogous studies. Results and conversation must remain unified without subsections. Your results must be immediately succeeded by your discussion.

The software utilized for imaging processes comprises Matlab and Python. The Otsu algorithm facilitates the activation and merging of two outlines, while MicroDicom software enables the measuring of the tumor area. The endeavor necessitates the utilization of segmented MRI images to accurately delineate the precise tumor region in each specimen. The methodology employs microdicom, active contour, Otsu, and the integration of two techniques to provide Axial T1 Contracts-type MRI pictures of 256x256 pixels. The algorithm has been employed to derive the findings in this context. The computation of mistakes can be conducted utilizing the algorithm detailed below:

Results Algorithm Error

Table 1 Calculation of Absolute Error Utilizing Numerical Methods

Fundamental Value					
No	Ground Truth	Active Contour	Microdicom	Otsu	Merge Method
1	357	1008	691	209	340
Error Absolut					
		Active Contour	Microdicom	Otsu	Merge Method
		-651	-334	148	17

The absolute error calculation in Table 1 is derived from the numerical method. The value is derived by the use of the ground truth generation process, active contour technique, MicroDicom viewer, Otsu method, and concluding with the merge two process. The fundamental value is derived from the application of diverse techniques to the segmentation of glioma MRI images. Upon acquisition, the value is adjusted to determine the absolute error between the reference value and the actual value. The table indicates that the merge two approach yields the smallest error value, but the active contour method results in the largest value. The hybrid approach integrates the Otsu method with the active contour method.

Table 2 Calculation of Relative Error Utilizing Numerical Methods

Fundamental Value					
No	Ground Truth	Active Contour	Microdicom	Otsu	Merge Method
1	357	1008	691	209	340
Error Absolut					

Active Contour	Microdicom	Otsu	Merge Method
182%	94%	41%	5%

Determine the relative error utilizing the numerical method presented in table 2. The value is derived from employing the ground truth construction process, active contour technique, MicroDicom viewer, Otsu method, and merging two processes. The fundamental value is derived from the examination of glioma MRI image slices employing diverse approaches. Upon obtaining the value, the error value is calculated by scaling the discrepancy between the fundamental value and the relative error. The merge two strategy exhibits the lowest error value in the table, whereas the active contour method demonstrates the highest value. The hybrid approach integrates the Otsu method with the active contour method. The resultant merged value is the percentage error, which is 5%.

Table 3 Percentage Computation Utilizing Numerical Methodology

Fundamental Value					
No	Ground Truth	Active Contour	Microdicom	Otsu	Merge Method
1	357	1008	691	209	340
Error Absolut					
		Active Contour	Microdicom	Otsu	Merge Method
		282%	194%	59%	95%

Determine the accuracy utilizing numerical methods based on the information presented in Table 3.3. The values are derived from the ground truth construction procedure, active contour technique, MicroDicom viewer, Otsu method, and a merging process. The fundamental value is derived from the analysis of various techniques used to glioma MRI images, particularly those acquired through image cropping. Upon achieving the target value, it is calculated by deducting the error value from the 100% accuracy, attained via reduction cropping. The outcome is dictated by the crop value, originally established at 100% and subsequently diminished to 95% in the merge two methodology. The maximum value is achieved through active contour computing.

a. *Template for Matching Results Algorithm*

This algorithm employs multiple techniques, including Otsu, active, and a merging of two methods, to evaluate and align the outcomes of image processing. Furthermore, this program compares the computation results derived from the Microdicom viewer application. This technique aims to detect images consisting of letters, numbers, symbols, and other applications related to image matching. To ascertain the defect status of the PCB image, a correlation value of 1 signifies an absence of flaws, whereas a correlation value of -1 denotes complete defects. The employed formula is:

$$r = \frac{\sum_{k=1}^N (x_{ik} - \bar{x}) \cdot (y_{jk} - \bar{y})}{\sqrt{\sum_{k=1}^N (x_{ik} - \bar{x})^2 \cdot \sum_{k=1}^N (y_{jk} - \bar{y})^2}}$$

The equation indicates that "r" represents the correlation coefficient, "xik" denotes the reference image, and "x̄" signifies the mean value of the reference image. Let y represent the input image, denote the mean of the input image, and let n signify the number of pixels in the image.

The provided equations facilitate the execution of an advanced two-way merging technique utilizing pixel capture units. This method can subsequently be enhanced by employing a template matching algorithm, which functions according to the following criteria:

- a) Contrast the outcomes of template matching with those of active contours.

$$r = \frac{\sum_{k=1}^{13}(2090 - 1389).(2601 - 1683)}{\sqrt{\sum_{k=1}^{13}(2090 - 1389)^2 . \sum_{k=1}^{13}(2601 - 1683)^2}} = -1$$

- b) Results of template matching utilizing MicroDicom

$$r = \frac{\sum_{k=1}^{13}(2090 - 1389).(8806 - 4908)}{\sqrt{\sum_{k=1}^{13}(2090 - 1389)^2 . \sum_{k=1}^{13}(8806 - 4908)^2}} = -1$$

- c) The outcomes pertain to template matching with Otsu's approach.

$$r = \frac{\sum_{k=1}^{13}(2090 - 1389).(1748 - 1311)}{\sqrt{\sum_{k=1}^{13}(2090 - 1389)^2 . \sum_{k=1}^{13}(1748 - 1311)^2}} = -1$$

- d) Utilizes a combination of two template matching techniques for matching objectives.

$$r = \frac{\sum_{k=1}^{13}(2090 - 1389).(2084 - 1360)}{\sqrt{\sum_{k=1}^{13}(2090 - 1389)^2 . \sum_{k=1}^{13}(2084 - 1360)^2}} = 1$$

The preliminary segmentation and extraction processes have been finalized. Processing employs a pixel-based methodology, commencing with the application of ground truth, Otsu's method, active contours, and the merging of two contours for analysis. Moreover, inaccuracies in the algorithmic computations are mitigated through the utilization of both abstract and relative numerical approaches. Tumor area matching is accomplished by a template matching algorithm, resulting in the use of template matching. Moreover, the template approach attains superior performance on merge two methods when the coefficient value is +1, exceeding the ideal value of the preceding technique

Acknowledgements

The authors wish thank to the Universitas Bhayangkara Jakarta Raya, The Republic of Indonesia, who supports it with full funding under the scheme of Research

References

- Bangare, S. L., Pradeepini, G., & Patil, S. T. (2017). Brain tumor classification using mixed method approach. 2017 International Conference on Information Communication and Embedded Systems, ICICES 2017, Icices, 0–3. <https://doi.org/10.1109/ICICES.2017.8070748>
- Ben Abdallah, M., Blonski, M., Wantz-Mezieres, S., Gaudeau, Y., Taillandier, L., & Moureaux, J. M. (2016). Predictive models for diffuse low-grade glioma patients under chemotherapy. Proceedings of the Annual International Conference of the IEEE Engineering in Medicine and Biology Society, EMBS, 2016-Octob, 4357–4360. <https://doi.org/10.1109/EMBC.2016.7591692>
- Example, P. (n.d.). pixels to centimeters calculator.
- Faria, A. V., Liang, Z., Miller, M. I., & Mori, S. (2017). Brain MRI pattern recognition translated to clinical scenarios. *Frontiers in Neuroscience*, 11(OCT), 1–14. <https://doi.org/10.3389/fnins.2017.00578>
- Feldman, J. P., Goldwasser, R., Mark, S., Schwartz, J., & Orion, I. (2014). Quantitative Methods Inquires 455 A MATHEMATICAL MODEL FOR TUMOR VOLUME EVALUATION USING TWO-DIMENSIONS. November 2008.
- Finch, A., Solomou, G., Wykes, V., Pohl, U., Bardella, C., & Watts, C. (2021). Advances in research of adult gliomas. *International Journal of Molecular Sciences*, 22(2), 1–36. <https://doi.org/10.3390/ijms22020924>
- Gong, K., Shi, T., Zhao, L., Xu, Z., & Wang, Z. (2021). Comparing the inter-observer reliability of the Tada formula among neurosurgeons while estimating the intracerebral haematoma volume. *Clinical Neurology and Neurosurgery*, 205(April), 106668. <https://doi.org/10.1016/j.clineuro.2021.106668>
- Gunawan, W., Suhartono, D., Purnomo, F., & Ongko, A. (2018). Named-Entity Recognition for Indonesian Language using Bidirectional LSTM-CNNs. *Procedia Computer Science*. <https://doi.org/10.1016/j.procs.2018.08.193>
- Hadi, H. P., Faisal, E., & Rachmawanto, E. H. (2022). Brain tumor segmentation using multi-level Otsu thresholding and Chan-Vese active contour model. *Telkomnika (Telecommunication Computing Electronics and Control)*, 20(4), 825–833. <https://doi.org/10.12928/TELKOMNIKA.v20i4.21679>
- Hasan, D., Nikoubashman, O., Pjontek, R., Stockero, A., Hamou, H. A., & Wiesmann, M. (2022). MRI appearance of chronic subdural hematoma. *Frontiers in Neurology*, 13. <https://doi.org/10.3389/fneur.2022.872664>
- Hashemi, N. S., & Aghdam, R. B. (2016). Template Matching Advances and Applications in Image Analysis. <http://arxiv.org/abs/1610.07231>
- Irianto, S. Y., Karnila, S., & Yuliawati, D. (2024). Study of Manhattan and Region Growing Methods for Brain Tumor Detection. *Journal of Advances in Information Technology*, 15(2), 183–194. <https://doi.org/10.12720/jait.15.2.183-194>
- Iskhakov, A. R. (2016). Mathematical Methods of Modeling of Image Processing and Analysis in the Modified Descriptive Algebras of Images. *Journal of Computational and Engineering Mathematics*, 3(1), 3–9. <https://doi.org/10.14529/jcem160101>
- Isunuri, B. V., & Kakarla, J. (2019). Brain Tumor Extraction using Adaptive Threshold Selection Network. 2019 IEEE 1st International Conference on Energy, Systems and Information Processing, ICESIP 2019, 1–6. <https://doi.org/10.1109/ICESIP46348.2019.8938318>

- Jolink, W. M. T., Lindenholtz, A., van Etten, E. S., van Nieuwenhuizen, K. M., Schreuder, F. H. B. M., Kuijf, H. J., van Osch, M. J. P., Hendrikse, J., Rinkel, G. J. E., Wermer, M. J. H., & Klijn, C. J. M. (2020). Contrast leakage distant from the hematoma in patients with spontaneous ICH: A 7 T MRI study. *Journal of Cerebral Blood Flow and Metabolism*, 40(5), 1002–1011. <https://doi.org/10.1177/0271678X19852876>
- Jones, P. W., & Rabbani, M. (2020). Digital Image Compression. *Digital Image Processing Methods*, December, 261–325. <https://doi.org/10.1201/9781003067054-8>
- Kumar, A., & Tiwari, A. (2019). A Comparative Study of Otsu Thresholding and K-means Algorithm of Image Segmentation. *International Journal of Engineering and Technical Research (IJETR)*, 9(5), 12–14. <https://doi.org/10.31873/ijetr.9.5.2019.62>
- Kumari, G. V., Prakash, M. S., Prasad, P. S., Srinivas, B., & Lavanya, B. (2020). Image Compression using Clustering Techniques for Bio Medical Applications. *International Journal on Emerging Technologies*, 11(3), 1185–1193. www.researchtrend.net
- Le Fèvre, C., Sun, R., Cebula, H., Thiery, A., Antoni, D., Schott, R., Proust, F., Constans, J. M., & Noël, G. (2022). Ellipsoid calculations versus manual tumor delineations for glioblastoma tumor volume evaluation. *Scientific Reports*, 12(1), 1–9. <https://doi.org/10.1038/s41598-022-13739-4>
- Madhupriya, G., Guru Narayanan, M., Praveen, S., & Nivetha, B. (2019). Brain tumor segmentation with deep learning technique. *Proceedings of the International Conference on Trends in Electronics and Informatics, ICOEI 2019*. <https://doi.org/10.1109/icoei.2019.8862575>
- Maeda, A. K., Aguiar, L. R., Martins, C., Bichinho, G. L., & Gariba, M. A. (2013). Hematoma volumes of spontaneous intracerebral hemorrhage: The ellipse (ABC/2) method yielded volumes smaller than those measured using the planimetric method. *Arquivos de Neuro-Psiquiatria*, 71(8), 540–544. <https://doi.org/10.1590/0004-282X20130084>
- Mehmet Kocak. (2022). Disadvantages of MRI. University Medical Center. <https://www.merckmanuals.com/home/special-subjects/common-imaging-tests/magnetic-resonance-imaging-mri>
- Mittal, K., Shekhar, A., Singh, P., & Kumar, M. (2017). Brain Tumour Extraction using Otsu Based Threshold Segmentation. *International Journal of Advanced Research in Computer Science and Software Engineering*, 7(4), 159–163. <https://doi.org/10.23956/ijarcsse/v7i4/0145>
- Müller, H., Michoux, N., Bandon, D., & Geissbuhler, A. (2004). A review of content-based image retrieval systems in medical applications - Clinical benefits and future directions. *International Journal of Medical Informatics*, 73(1), 1–23. <https://doi.org/10.1016/j.ijmedinf.2003.11.022>
- Numerical Methods 5.1. Introduction. (1998). *New England Journal of Medicine*, 339(24), 1725–1733. <http://www.nejm.org/doi/abs/10.1056/NEJM199812103392401>
- Parihar, A. S. (2018). A study on brain tumor segmentation using convolution neural network. *Proceedings of the International Conference on Inventive Computing and Informatics, ICICI 2017*. <https://doi.org/10.1109/ICICI.2017.8365336>
- Parney, I. F., & Prados, M. D. (2005). Glioblastoma multiforme. *Textbook of Neuro-Oncology*, 143–148. <https://doi.org/10.1016/B978-0-7216-8148-1.50022-X>
- Parveen, & Singh, A. (2015). Detection of brain tumor in MRI images, using combination of fuzzy c-means and SVM. *2nd International Conference on Signal Processing and Integrated Networks, SPIN 2015*, 98–102. <https://doi.org/10.1109/SPIN.2015.7095308>

- Sápi, J., Kovács, L., Drexler, D. A., Kocsis, P., Gajári, D., & Sápi, Z. (2015). Tumor volume estimation and quasi- continuous administration for most effective bevacizumab therapy. *PLoS ONE*, 10(11), 1–20. <https://doi.org/10.1371/journal.pone.0142190>
- Sasvari, P. (2013). The Effects of Technology and Innovation on Society. <http://arxiv.org/abs/1307.3911>
- Shukran, M. A. M., Abdullah, M. N., & Yunus, M. S. F. M. (2021). New Approach on the Techniques of Content-Based Image Retrieval (CBIR) Using Color, Texture and Shape Features. *Journal of Materials Science and Chemical Engineering*, 09(01), 51–57. <https://doi.org/10.4236/msce.2021.91005>
- Skaržauskienė, A., Tamošiūnaitė, R., & Žalėnienė, I. (2013). Defining Social Technologies. In: *Proceedings of the European Conference on Information Management & Evaluation*, 1, 239–247. <http://web.ebscohost.com/ehost/pdfviewer/pdfviewer?vid=4&sid=5eaa0323-337e-4913-a9a3-ac95549e54f9%40sessionmgr112&hid=121>
- Sreenivasan, S., Madhugiri, V., Sasidharan, G., & Kumar, R. V. R. (2016). Measuring glioma volumes: A comparison of linear measurement based formulae with the manual image segmentation technique. *Journal of Cancer Research and Therapeutics*, 12(1), 161–168. <https://doi.org/10.4103/0973-1482.153999>
- Swati, Z. N. K., Zhao, Q., Kabir, M., Ali, F., Ali, Z., Ahmed, S., & Lu, J. (2019). Content-Based Brain Tumor Retrieval for MR Images Using Transfer Learning. *IEEE Access*, 7, 17809–17822. <https://doi.org/10.1109/ACCESS.2019.2892455>
- Vaillant, M., & Davatzikos, C. (1997). Finding parametric representations of the cortical sulci using an active contour model. *Medical Image Analysis*, 1(4), 295–315. [https://doi.org/10.1016/S1361-8415\(97\)85003-7](https://doi.org/10.1016/S1361-8415(97)85003-7)
- Vauzia, V. V., & Sumitra, I. D. (2020). Technology of Health Services in Industrial Revolution 4.0 Era. *IOP Conference Series: Materials Science and Engineering*, 879(1), 0–6. <https://doi.org/10.1088/1757-899X/879/1/012012>
- Wang, Z., Li, B., & Li, L. (2019). Research on water quality detection technology based on multispectral remote sensing. *IOP Conference Series: Earth and Environmental Science*. <https://doi.org/10.1088/1755-1315/237/3/032087>
- Widodo, C. E., Adi, K., Sugiharto, A., Qidir Maulana, B. S., & Pamungkas, A. (2016). Volume target delineation for brain tumor in MRI images using active contour segmentation method. *International Journal of Applied Engineering Research*, 11(16), 9031–9036.
- Wongso, R., Meiliana, & Suhartono, D. (2017). A literature review of question answering system using Named Entity Recognition. *Proceedings - 2016 3rd International Conference on Information Technology, Computer, and Electrical Engineering, ICITACEE 2016*. <https://doi.org/10.1109/ICITACEE.2016.7892454>
- Yang, G., Nawaz, T., Barrick, T. R., Howe, F. A., & Slabaugh, G. (2015). Discrete Wavelet Transform-Based Whole-Spectral and Subspectral Analysis for Improved Brain Tumor Clustering Using Single Voxel MR Spectroscopy. *IEEE Transactions on Biomedical Engineering*, 62(12), 2860–2866. <https://doi.org/10.1109/TBME.2015.2448232>